






Article

Influence of Extrusion Temperature on the Corrosion Behavior in Sodium Chloride Solution of Solid State Recycled Aluminum Alloy 6061 Chips

Nabeel H. Alharthi ^{1,*}, El-Sayed M. Sherif ^{2,3} , Mohamed A. Taha ⁴ , Adel T. Abbas ¹ ,
Hany S. Abdo ^{2,5}  and Hamad F. Alharbi ¹ 

¹ Department of Mechanical Engineering, College of Engineering, King Saud University, P.O. Box 800, Riyadh 11421, Saudi Arabia; aabbas@ksu.edu.sa (A.T.A.); harbihf@ksu.edu.sa (H.F.A.)

² Centre of Excellence for Research in Engineering Materials, King Saud University, P.O. Box 800, Riyadh 11421, Saudi Arabia; esherif@ksu.edu.sa (E.-S.M.S.); habdo@ksu.edu.sa (H.S.A.)

³ Electrochemistry and Corrosion Laboratory, Department of Physical Chemistry, National Research Centre, El-Beboth St. 33, Dokki, Cairo 12622, Egypt

⁴ Department of Mechanical Design and Production, Faculty of Engineering, Zagazig University, Zagazig 44519, Egypt; eng_mohamed_2017@yahoo.com

⁵ Mechanical Design and Materials Department, Faculty of Energy Engineering, Aswan University, Aswan 81521, Egypt

* Correspondence: alharthy@ksu.edu.sa

Received: 17 March 2020; Accepted: 23 April 2020; Published: 29 April 2020



Abstract: In the present work, aluminum alloy 6061 (AA6061) device chips were subjected to cold compaction monitored by an extrusion procedure at an extrusion ratio of 5:2 and elevated temperatures of 350, 425, and 500 °C, respectively. The influence of changing temperature on the corrosion of the extruded alloys after 1 h and 24 h in 3.5% NaCl solutions was studied. The polarization (cyclic potentiodynamic polarization, CPP) results indicated that the corrosion decreases with the increase of extrusion temperature of AA6061 from 350 to 500 °C. Impedance (electrochemical impedance spectroscopy, EIS) experiments provided a remarkable increase in the corrosion resistance with rising the extrusion temperature. Potentiostatic current-time (PCT) curves indicated that the current initially increased then decreased for all alloys after 1 h measurements. Prolonging the exposure time to 24 h was observed to decrease the rate of corrosion for all AA6061 alloys as proved by CPP and EIS data. This effect was found to increase the pitting corrosion as indicated by the measured PCT curves and by the scanning electron microscopy (SEM) images for the surface of the alloys. The surface layers formed on AA6061 alloys were mostly composed of aluminum oxide as presented by the spectra of the energy dispersive X-ray analyzer (EDX). All results indicated that the increase of the temperature of extrusion increased the corrosion resistance via decreasing the corrosion current and corrosion rate, and that this effect was found remarkably increased when the immersion time increased from 1 to 24 h exposure to the chloride test solution.

Keywords: aluminum alloy 6061; corrosion; extrusion; solid state; recycled aluminum chips

1. Introduction

Aluminum and its alloys have become a better alternative and an economic competitor in engineering applications as well as the recycling of the chips of aluminum alloy without melting. Nowadays, the possibility of recycled aluminum chips gives these alloys an edge and conveys a new square for aluminum foundries. Chips reprocessing needs an efficient pre-treatment procedure that depends on the optimization of consolidation techniques to obtain higher high-quality metal recovery

rates. This will in turn reduce the recycling. Aluminum recycling through hot extrusion processes is one of the main techniques used for recycling of aluminum chips without the need for a melting process. A characteristic behavior of aluminum to avoid oxidation can be identified as the formation of an invisible oxide layer on its surface when exposed to the ambient air [1,2]. This layer prevents further oxidation of the metal and acts as a protective layer. This is the reason aluminum is known for its high corrosion resistance property [1–4]. External factors may destroy this protective layer and aluminum is thus prone to further oxidation [2]. Otherwise, aluminum is considered to be highly resistant to all types of atmospheres that often corrode other metals.

The behavior of corrosion for AA6061 aluminum alloy in various corrosive environments was studied by many researchers [5–11]. Rangasamy et al [5] investigated the effect of La_2O_3 in aluminum alloys. Shahidi and Gholamhosseinzadeh [6] presented a study on the corrosion resistance of Aluminum alloy AA6061 with citric acid along with NaCl using different techniques. Rosliza and Nik [7] studied the effect of using tapioca starch to enhance the corrosion resistance of AA6061 alloy using different polarization techniques and electrochemical impedance measurements. The inhibition of seawater corrosion for AA6061 aluminum alloys using sodium benzoate has been carried out [9]. Dadvand et al [10] studied the effect of coating AA6061 alloys with electroless nickel-phosphorus on the corrosion resistance of the alloy. They concluded that a general increase in phosphorus content is associated with an increase in the corrosion resistance. They correlated their results to the fact of activating and inhibiting of phosphorus on corrosion resistance. The activating effect is explained by the thin layer produced with low P content that is incapable of protecting the alloy, while when P content increases, the inhibiting effect increases as a result of phosphate formation. Linardi et al [12] investigated the effect of storing components manufactured using AA6061 aluminum alloys in demineralized water basins. Immersion tests on AA6061 alloy alloys were performed along a variety of duration ranging from three days all the way up to a lengthy period of four months. Oxide samples are then analyzed and examined and they estimated the growth rate of oxides in different solutions.

The re-use of scraped aluminum was done along the past centuries but was given an important highlight in the 20th century era. The main objective of this recycling process was to create a more sustainable environment by making use of scrap material, aiding the reduction of harmful pollutants and the use of fewer new resources. The very high demand and high production cost of aluminum alloys is a justifiable cause for the importance of this research paper. Various manufacturing processes such as casting, machining, and material depositing are used to produce aluminum chips, which are the hardest to recycle among all types of aluminum scrap. Direct and indirect ways of recycling have been investigated in the literature [13,14]. It has been found that direct recycling methods are more efficient as they can make use of up to 95% of scraped aluminum, while conventional processes make use of only 50% of scrap in new products. In our pervious study [15], the effect of extrusion temperature on the roughness and time of machining for AA6061 alloy were reported using the Box–Behnken design. The study also investigated depth of cut, feed rate, and cutting speed as the machining parameters on the surface roughness of the machined specimens. In this work, the influence of increasing the extrusion temperature from 350 to 500 °C at the extrusion phase on the corrosion of the solid recycled alloys was studied. The effect of exposure periods of time on the corrosion of the tested materials was also reported.

2. Materials, Methods and Experiments

2.1. Manufacture of Chips

The starting material source for the proposed research was an AA6061 aluminum alloy having the following chemical compositions; 0.85% Mg, 0.80% Si, 0.48% Fe, 0.26% Cu, 0.051% Mn, 0.33% others, and the balance is Al (all in weight %) [15]. The device chips were prepared using dry conditions (under revolving) under optimized experimental following cutting settings; 88 m/min (i.e., cutting speed), 1 mm/rev (i.e., feed) and 1 mm (i.e., depth of cut). The device chips were cold compacted at

room temperature into cylindrical billets with the diameter and length of 25 and 35 mm, respectively. Thereby, the compacted billets were hot extruded into rods (with final diameter of 11 mm) through flat-face die with an extrusion ratio of 5.2 at prominent temperatures of 350, 425 and 500 °C.

2.2. Chemicals, Electrochemical Cell and Corrosion Experiments

A solution of 3.5% (weight %) NaCl was prepared from a pure sodium chloride salt, 99.0%, which was purchased from Sigma-Aldrich (Glasgow, UK). Corrosion experiments were carried out in an electrochemical cell with three-electrode setup with a platinum wire counter electrode (CE), AA6061 alloy as the working electrode (WE), which was in a cylindrical shape and Ag/AgCl as the reference electrode. The preparation of WE was carried out by welding a copper rod to the cylindrical Al 6061 alloy, then the whole surface area was mounted using nonconductive epoxy, except the exposure surface which was the testing area. All experiments were collected on a fresh such that was polished by automatic polisher using fine metallographic emery paper (1200 grits) then washed with distilled water. The diameter of the testing surface of the working electrode was approximately 6 mm with a total exposed area of 28.3 mm².

The corrosion performance of AA6061 alloys corresponding to the as received and the extruded ones at 350, 425 and 500 °C were reported. The electrochemical data were collected after 1 h and 24 h and were carried out using an Autolab PGSTAT20 machine. The polarization curves were obtained between −1200 and −250 mV and then from −250mV in the reverse direction till the backward current intersects with the forward current. The scan rate was the same for all CPP experiments at 0.167 mVs^{−1}. The EIS measurements were gathered at OCP value with frequency starts from 100 kHz to 100 mHz with an ac wave of ±5 mV peak-to-peak overlaid on a dc bias potential. The impedance data were obtained at a rate of 10 points per decade change in frequency using PowerSINE software (Metrohm, Amsterdam, The Netherlands). All measurements were carried out in triplicate in open to air solutions and at room temperature.

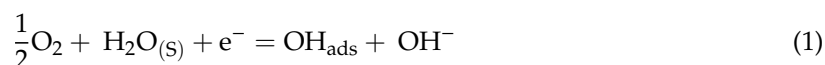
A SEM type JSM7600F (JEOL, Tokyo, Japan) was utilized to analyze the alloys surface morphology studies in terms of surface roughness and corrosion products. The EDX profiles were analyzed using an EDX unit attached to the SEM microscopy.

3. Results and Discussions

3.1. CPP Measurements

The obtained CPP curves for the as received are shown in Figure 1a, and the extruded alloys at 350, 425, and 500 °C in NaCl solutions after 1 h are shown in Figure 1b–d, respectively. The CPP plots after 24 h are seen in Figure 2. The corrosion parameters here are the cathodic (β_c) and anodic (β_a) Tafel slopes, corrosion rate (K_{Corr}), corrosion potential (E_{Corr}), pitting corrosion (E_{Pit}), the potential difference $E_{Pit}-E_{Corr}$, polarization resistance (R_p), and corrosion current density (j_{Corr}) and their values are in Table 1. The Tafel slopes were simply obtained, by drawing two tangents, one to touch the maximum number of points of the Tafel line of the cathode to obtain the values of β_c , and the other tangent to touch the maximum number of points of the Tafel line of anode to obtain the values of β_a . The values of E_{Corr} and j_{Corr} were obtained from the intersection of the two tangents. Furthermore, K_{Corr} and R_p values were got as per the footnote of Table 1 [3].

The reaction of the cathodic branch for Al and its alloys in NaCl solution is the reduction of oxygen as follows [1]:



The adsorption of the reduced oxygen also occurs as per the following reaction:



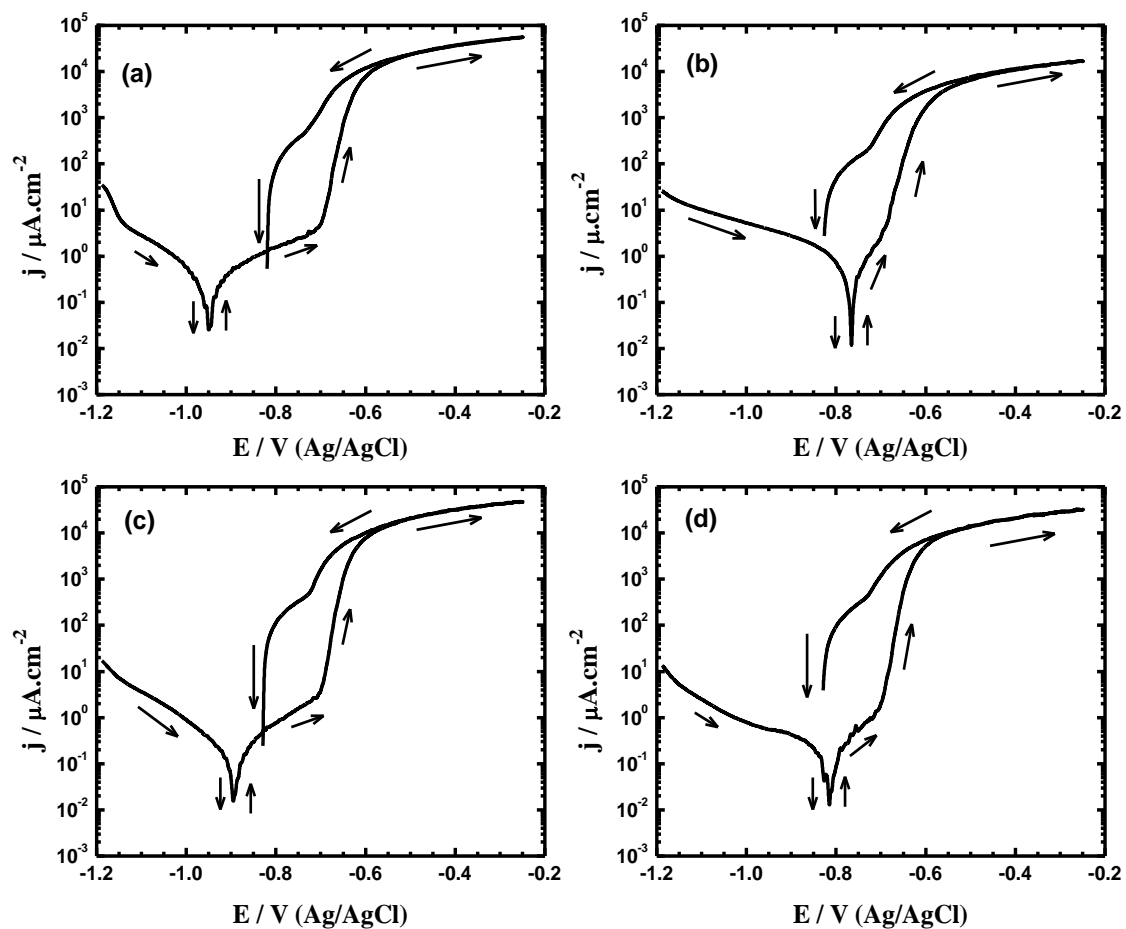
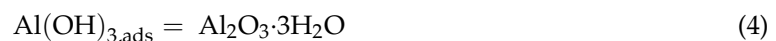
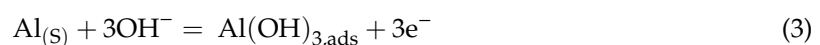


Figure 1. Polarization of AA 6061 alloys, (a) the as received and the extruded alloys (b) 350, (c) 425, and (d) 500 °C, after immersion in 3.5% NaCl solutions for 1 h.

The anodic reaction takes place on the surface of Al alloys via the formation of Al_2O_3 , which transforms to $\text{Al}_2\text{O}_3 \cdot 3\text{H}_2\text{O}$ [3];



Figures 1 and 2 reveal that the cathodic branch starts via decreasing the current towards the values of j_{Corr} and then increases in the anodic side. This increase in the current values slightly slows down with scanning the potential as a result of Al_2O_3 formation, which causes a surface protection. The current then increases again by the dissolution of the formed oxide film and the occurrence of pitting corrosion via increasing the applied potential and the aggressiveness action of Cl^- . Reversing potential in the backward scanning is seen to increase the current values, particularly after long immersion time (Figure 2). This is mostly due to the effect of pitting corrosion that took place and was confirmed by the appearance of a hysteresis loop. Here, the dissolution of Al takes place via its oxidation to Al^{3+} according to this reaction:



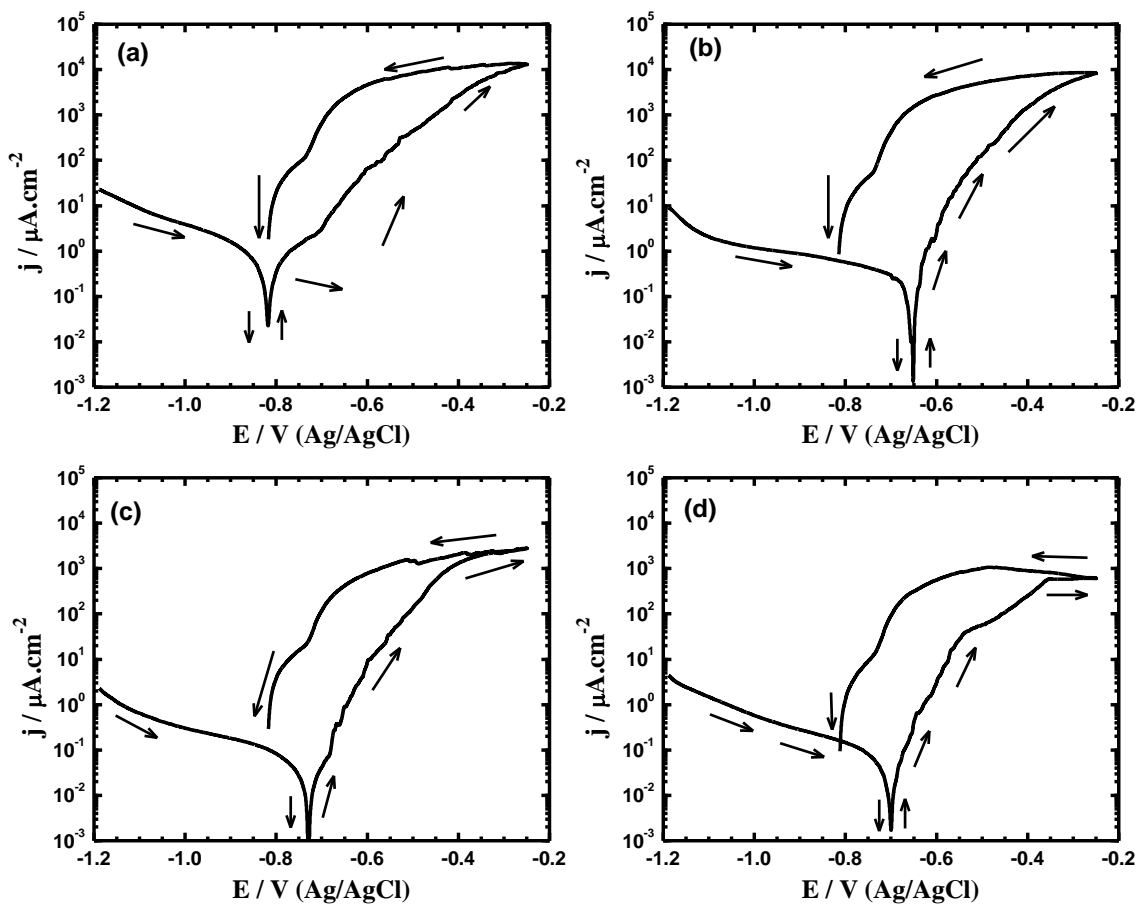
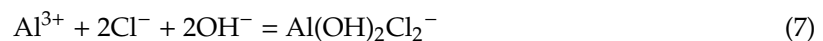


Figure 2. Cyclic potentiodynamic polarization (CPP) curves for AA 6061 alloys, (a) the as received and the extruded alloys at (b) 350, (c) 425, and (d) 500 °C, respectively after 24 h immersion in 3.5% NaCl solutions.

According to the reported results [1,3,16–21], a view presumed a barrier of AlCl_3 salt is formed inside the pits when it is initially formed. The pitting corrosion then takes place after the formation of AlCl_4^- . This aluminum chloride complex diffuses into the bulk of the solution as follows:



Another vision claimed that the aggressiveness action of the chloride ions comes from its ability to be adsorbed and then react with aluminum cations, Al^{3+} , which in turn could lead to the formation of a chloride complex as follows [1,3]:



Here, extruding AA 6061 alloy at 350 °C led to reducing j_{Corr} and K_{Corr} values, while increased the value of R_p as shown in Table 1. The corrosion resistance, R_p , increases with the increase of the temperature of extrusion; i.e., 500 °C > 425 °C > 350 °C > the as received alloy. Increasing the extrusion temperature to higher value of 425 °C and further to 500 °C led to further decreases in the corrosion parameters [22].

In order to report the effect of prolonging the period of exposure of time to 24 h on the behavior of corrosion for the extruded AA 6061 alloy at different temperatures, the CPP measurements were carried out as shown in Figure 2. The data measured and depicted by Figure 1 as well as Figure 2 with the parameters listed in Table 1 indicated that prolonging the time of immersion to 24 h decreased the values of j_{Corr} and K_{Corr} and increased the values of R_p for all tested alloys. The good corrosion

resistances gained for the recycled alloys in compared to the as received alloy is due to the absence of voids and the strong bonding between individual chips for the extruded alloys and that effect increases with the increase of the extrusion temperature [13,21]. Moreover, the higher corrosion resistance of the recycled alloy at 500 °C, is related to the combined effects of the grain refinement as compared with the as-received alloy, oxide contaminants from the scraps, and the higher extrusion temperature [21–25]. The fine-grained microstructure is caused by severe plastic strain imposed during machining and recycling [24,25]. In addition, the plastic strain and conditions of hot temperature and pressure led to the broken of oxide layers into particles. Both grain refinement and oxide contaminant play a vital role as a corrosion barrier [26–28]. It has been reported also that the higher temperature increases the bonding between chips and reduces the percentage of voids [24,29]. Similar observations were obtained by Chino et al. [27] where, the corrosion resistance of solid state recycled AZ31Mg alloy and pure Mg chips were superior as compared with those of as received alloy.

Table 1. Corrosion data gathered from polarization curves of Al alloys in the chloride solutions.

Alloy	Parameter							
	$\beta_c/\text{mVdec}^{-1}$	$E_{\text{Corr}}/\text{mV}$	$\beta_a/\text{mVdec}^{-1}$	$j_{\text{Corr}}/\mu\text{A}\cdot\text{cm}^{-2}$	E_{Pit}/mV	$E_{\text{Pit}}-E_{\text{Corr}}/\text{mV}$	${}^a R_p/\text{k}\Omega\cdot\text{cm}^2$	${}^b K_{\text{Corr}}/\text{mpy}$
As-received AA6061 (1 h)	130 ± 2	−955 ± 4	80 ± 2	0.45 ± 0.1	−695 ± 5	260 ± 5	47.849	0.0491
Extruded AA6061 at 350 °C (1 h)	110 ± 3	−950 ± 3	110 ± 4	0.30 ± 0.3	−690 ± 3	260 ± 3	86.353	0.00327
Extruded AA6061 at 425 °C (1 h)	120 ± 3	−890 ± 3	100 ± 2	0.25 ± 0.2	−690 ± 2	200 ± 2	94.682	0.00273
Extruded AA6061 at 500 °C (1 h)	140 ± 2	−820 ± 5	100 ± 3	0.20 ± 0.2	−685 ± 3	135 ± 3	126.812	0.00218
As-received AA6061 (24 h)	100 ± 3	−845 ± 5	95 ± 2	0.40 ± 0.2	−700 ± 4	145 ± 4	96.281	0.00436
Extruded AA6061 at 350 °C (24 h)	145 ± 2	−770 ± 3	65 ± 4	0.18 ± 0.4	−640 ± 2	130 ± 2	108.408	0.00196
Extruded AA6061 at 425 °C (24 h)	130 ± 3	−750 ± 2	63 ± 3	0.035 ± 0.04	−640 ± 5	110 ± 5	527.146	0.00038
Extruded AA6061 at 500 °C (24 h)	140 ± 3	−685 ± 4	55 ± 5	0.030 ± 0.01	−620 ± 3	65 ± 3	572.278	0.00033

^a Values of R_p were calculated from $R_p = \frac{1}{j_{\text{Corr}}} \left(\frac{\beta_c \cdot \beta_a}{2.3(\beta_c + \beta_a)} \right)$ [30]. ^b Values of K_{Corr} were calculated from $R_{\text{Corr}} = j_{\text{Corr}} \left(\frac{k \cdot E_W}{d \cdot A} \right)$ [30], where k is a constant to define the unit for K_{Corr} , the value of k is 3272 mm (amp^{−1} cm^{−1} year^{−1}), E_W is the equivalent weight of the Al alloy, the value of E_W is 9 gram equivalent), d is the density of the Al alloy, the value of d is 2.7 g cm^{−3}, and A is the surface area for the titanium alloy, the value of A is 1 cm².

3.2. EIS Measurements

The Nyquist plots for (1) the as received and the extruded at (2) 350, (3) 425 and (4) 500 °C AA 6061 alloys after their exposure to 3.5% NaCl solutions for 1 h and 24 h are proposed in Figures 3 and 4, respectively. These EIS data were fitted to the circuit model in Figure 5 and the values obtained from this circuit are summarized in Table 2. These values can be defined as; R_S is a solution resistance, R_p is a polarization resistance, and Q (Y_Q , CPEs) is constant phase elements [31–33].

The spectra of Figure 3 present only one semicircle whose diameter is the smallest for the as received alloy (spectrum 1). The diameter of the semicircle slightly increased when the recycled alloy was extruded at 350 °C as seen on spectrum 2. The extrusion at 425 °C, largely increased the width of the spectrum and the largest diameter was measured for the alloy that was extruded at 500 °C (curve 4). This behavior indicates that extruding AA6061 alloy at 350 °C increases its corrosion resistance and this effect remarkably enhanced when the temperature increases to 450 °C and further to 500 °C.

After 24 h exposure periods of time, the resistance to corrosion for the tested alloys increased. This is because immersing the alloy in NaCl solution for long period decreases the uniform corrosion because of corrosion product formation. The formation of such products and its accumulation on the alloy's surface with time reduces its corrosion. This effect increases with extruding the alloy at 350 °C and highly increases when temperature was 450 °C and further to 500 °C. Increasing the exposure time was found also to have positive impact on increasing the resistance to corrosion for all alloys. The increase of resistance with increasing temperature as well as the time of exposure was also confirmed by the values of R_S , R_p and Q as seen from Table 2. Here, the values of R_S and R_p increased for the extruded alloys, particularly when the temperature was raised to 450 and 500 °C.

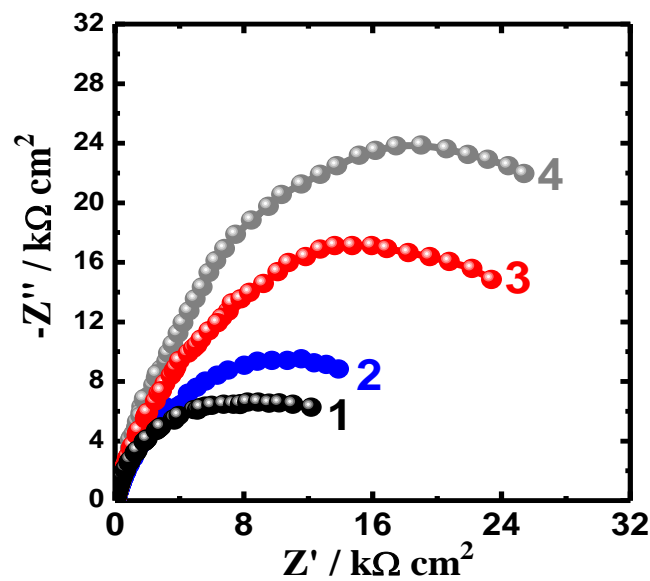


Figure 3. Nyquist spectra collected for 6061 alloys, (1) the as received and the extruded alloys at (2) 350, (3) 425, and (4) 500 °C, respectively after the immersion for 1 h in 3.5% NaCl solutions.

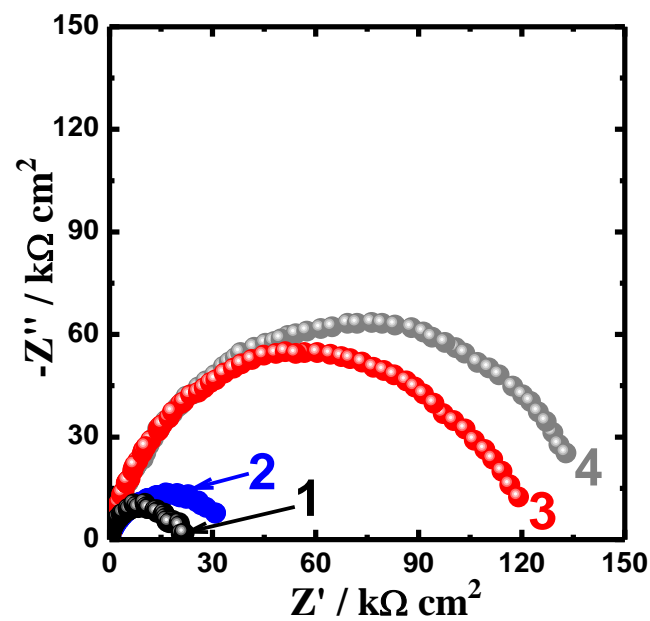


Figure 4. Nyquist spectra for 6061 alloys, (1) the as received and the extruded alloys at (2) 350, (3) 425, and (4) 500 °C after the immersion in 3.5% NaCl solutions for 24 h.

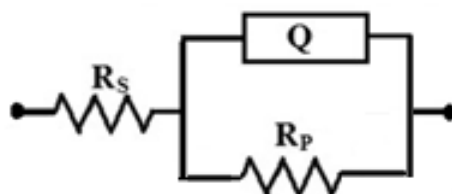


Figure 5. The circuit used in fitting the EIS experiments.

Moreover, the (CPEs), Q is considered as double layer capacitors as its corresponding n -values are varied from 0.86 to 0.94 for all alloys at the different conditions. Here, the values of Y_Q decrease with temperature and exposure time to 24 h. The decrease of Y_Q values indicates that the dissolution of AA6061 alloy decreases via decreasing mass loss of the alloy in NaCl solutions. The EIS data hence

agree with the obtained CPP measurements and both proved the advantages of rising the extrusion degree of temperature and the effect of increasing the exposure time on the improvement of resistance to corrosion of the recycled AA6061 alloys in the test solution.

Table 2. EIS results of AA6061 alloys in chloride solutions.

Alloy	EIS Parameters			
	$R_S / \Omega \text{ cm}^2$	Q		$R_{P1} / \Omega \text{ cm}^2$
		$Y_Q / \mu\text{F cm}^{-2}$	n	
As-received AA6061 (1 h)	19.35 ± 2.1	2759 ± 12	0.88 ± 0.2	8662 ± 18
Extruded AA6061 at 350 °C (1 h)	22.89 ± 1.8	1978 ± 9	0.87 ± 0.3	$16,940 \pm 20$
Extruded AA6061 at 425 °C (1 h)	24.63 ± 1.5	1581 ± 8	0.86 ± 0.2	$24,081 \pm 19$
Extruded AA6061 at 500 °C (1 h)	25.55 ± 3	1358 ± 8	0.86 ± 0.2	$32,893 \pm 22$
As-received AA6061 (24 h)	20.77 ± 2	834 ± 9	0.94 ± 0.1	$30,039 \pm 21$
Extruded AA6061 at 350 °C (24 h)	23.89 ± 1.7	688 ± 8	0.87 ± 0.3	$39,707 \pm 19$
Extruded AA6061 at 425 °C (24 h)	25.17 ± 2.5	591 ± 7	0.88 ± 0.2	$132,330 \pm 18$
Extruded AA6061 at 500 °C (24 h)	27.68 ± 3	533 ± 5	0.92 ± 0.1	$150,120 \pm 20$

3.3. PCT Experiments

The change of current vs. time at a constant potential value measurement was performed in order to further understand the corrosion of the different AA6061 alloys and whether pitting would take place in the test solution. The PCT technique has been employed to investigate the corrosion of various materials in various media [30,34–36]. Figure 6 shows the PCT curves collected at -680 mV for the different 6061 alloys after their immersion for 1.0 h in the 3.5% NaCl solutions, (1) the as received, and the extruded alloys at (2) 350, (3) 425, and (4) 500 °C, respectively. It is clear from Figure 6 that the initial current for all alloys increases rapidly in the first few minutes of the measurement.

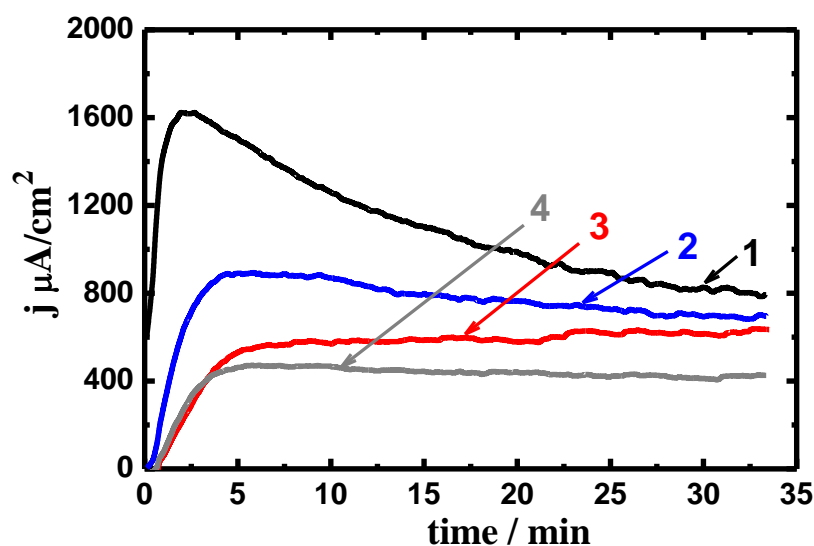


Figure 6. PCT curves gathered at -680 mV for 6061 alloys, (1) the as received and the extruded alloys at (2) 350, (3) 425, and (4) 500 °C after their immersion in 3.5% NaCl solutions for 1.0 h.

For the as received alloy, after its initial current increases and reaching the maximum values, it slightly decreased with time until reaching the end of the run. Highest absolute current values were recorded for the as received alloy. For the extruded AA6061 alloy at 350 °C, the current-time behavior was almost same but at much lower absolute current values. Raising the temperature to 425 °C for the alloy lowered the values of current with time and the minimum values of current were recorded for the extruded alloy at 500 °C. It is thus proved that raising the extruding temperature decreases the uniform

attack for all recycled alloys here. This effect also allows the alloy to have pitting corrosion since the recorded currents for the extruded alloys at 425 and 500 °C did not decrease with time, although it was the lowest.

The increase of time to 24 h before measurement (Figure 7) decreased the initial current to be almost zero. This is because the corrosion products accumulated onto the surface of the alloys and thus provided an initial passivation to the alloys. The current gradually increases with time for all alloys as a result of the breakdown of the corrosion products under applied potential and the corrosive effect of the test solution. The shift of the current with time was greatest for the as received alloy followed by the extruded alloy at 350 °C. The extruded alloys at 425 and 500 °C recorded almost the same behavior but with lower current values, which indicates that the increase of extrusion temperature even after 24 h immersion in the chloride solution decreases the uniform corrosion of AA6061 recycled alloy. The current-time behavior obtained of all alloys after 24 h confirms that these alloys suffer pitting corrosion at this condition and agreed with the results obtained by CPP and EIS data.

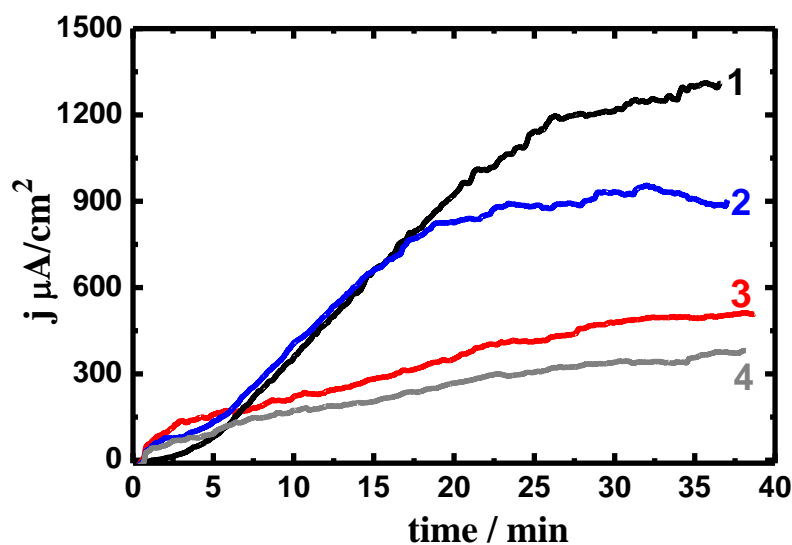


Figure 7. PCT curves gathered at -680 mV for 6061 alloys, (1) the as received and the extruded alloys at (2) 350, (3) 425, and (4) 500 °C after their immersion in 3.5% NaCl solutions for 24 h.

3.4. SEM Micrographs and EDX Profile Analyses

The surface morphology as well as elemental analysis for all alloys after being immersed for 24 h and having an applied -680 mV for 40 min were carried out via SEM and EDX examinations, respectively. Figure 8 presents the micrograph of SEM and EDX spectrum for the as received AA6061 alloy after its immersion in NaCl solution for 24 h before fixing an amount of -680 mV for 40 min. Similar images and spectra were also obtained for the extruded alloys at 425 and 500 °C as seen in Figures 9 and 10, respectively. The SEM micrograph of Figure 8 of the as received AA6061 alloy indicated that the surface has many propagated pits surrounded by corrosion products. The EDX spectrum taken for the surface of the as received AA6061 alloy confirms that the surface has the following weight percentages (wt %); 77.51% Al, 18.98% O, 2.38% Si, 0.56% Mg, 0.20% Na, and 0.38% Cl. The high percent of Al and O indicate that the main compound that was existed on the surface of the alloy is an oxide that is mostly Al_2O_3 . The low percent of Cl and Na reveal that a little NaCl salt was deposited on the surface.

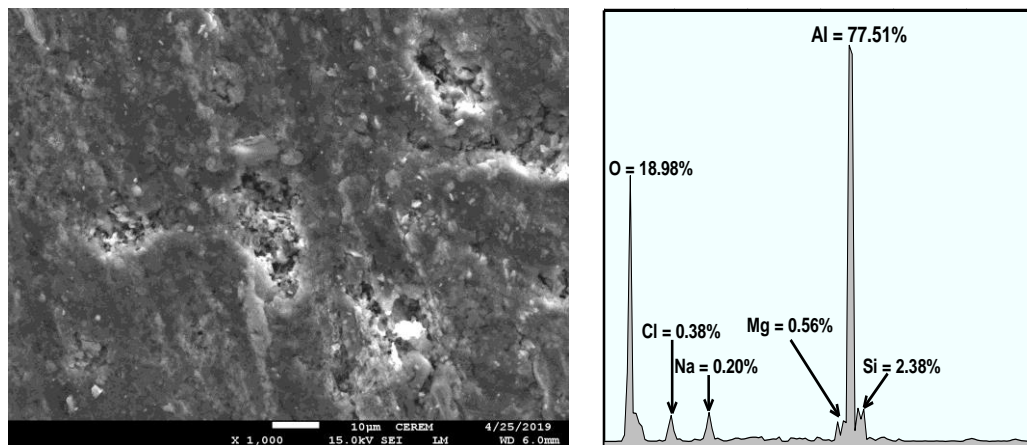


Figure 8. SEM micrograph and EDX profile analysis taken for the as received alloy after its immersion for 24 h in NaCl solution and applying -680 mV for 40 min.

The SEM image and the EDX spectrum taken from the surface of the extruded alloys at 350 °C after 24 h exposure in NaCl before applying an amount of -680 mV are depicted in Figure 9. It is declared from Figure 9 that this alloy has a possible pitting corrosion. The presence of pits on the as received alloy and the alloy that was extruded at 350 °C confirms the current vs. time behavior, Figure 7 (curve 1 and curve 2). This also reveals that the as received alloy and the alloy that was extruded at 350 °C have similar mechanisms. The EDX spectrum taken for the surface of the alloy extruded at 350 °C confirms that the surface has the following wt %; 63.38% Al, 29.32% O, 3.63% Si, 1.27% Fe, 0.28% Mg, 0.71% Na, and 1.40% Cl. It is indicated from the high percent of Al and O confirms the presence of Al_2O_3 on the surface of the alloy. There is also a slightly thinly deposited film forming the solution onto the surface of the alloy, as indicated by the presence of the low percent of both Na and Cl. Other elements found on the surface of the alloy that was extruded at 350 °C are from the main contents of AA6061 alloy.

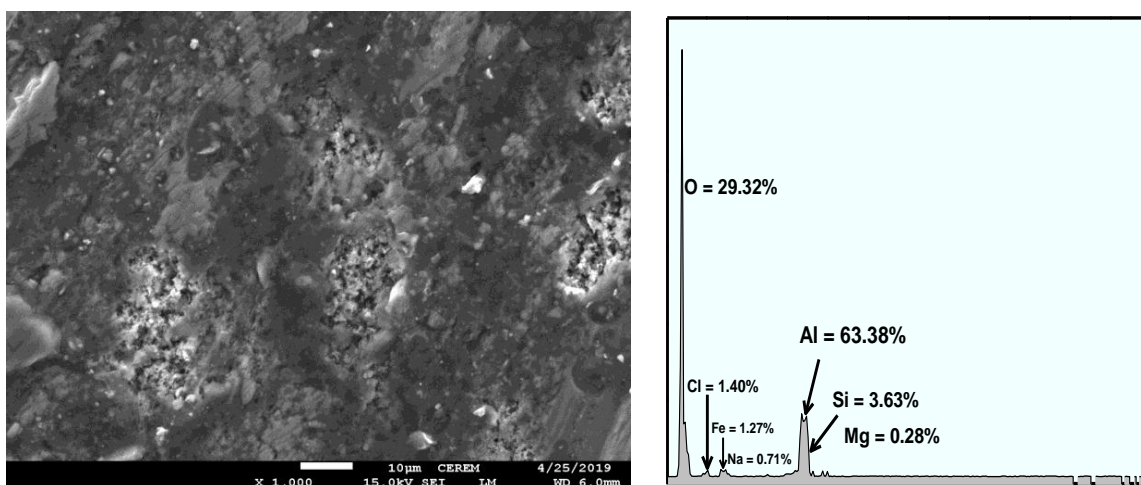


Figure 9. SEM and EDX for the recycled alloy that was extruded at 350 °C after 24 h exposure to NaCl solution at -680 mV that was applied for 40 min.

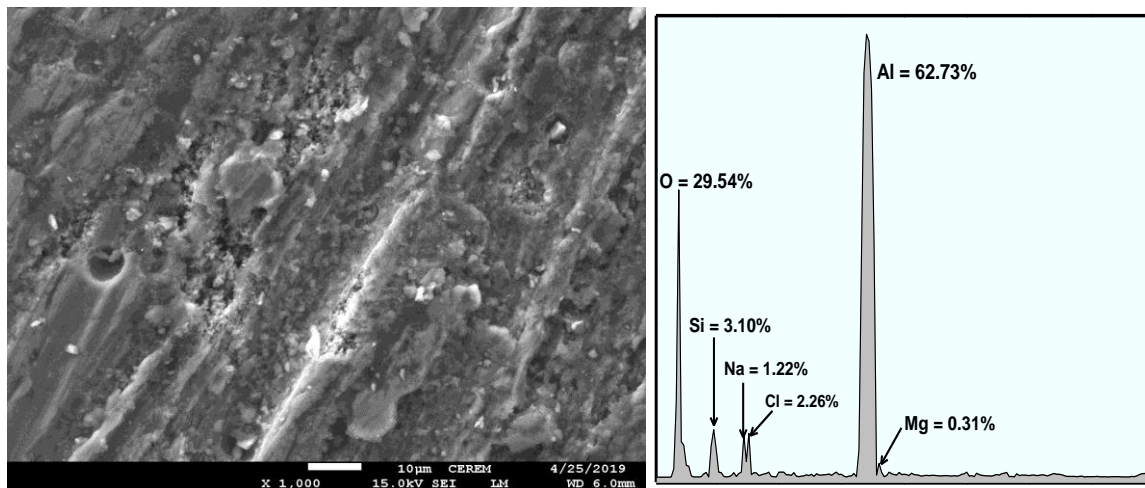


Figure 10. The SEM and EDX investigations for the alloy that was extruded at 500 °C after 24 h exposure in NaCl solution at –680 mV that was applied for 40 min.

The surface investigation (SEM/EDX) for the alloy that was extruded at 500 °C after 24 h exposure in NaCl solution before stepping a value of –680 mV for 40 min are depicted in Figure 10. It is obvious that the surface of the alloy that was extruded at 500 °C developed thicker layer of corrosion product that could protect the alloy from being more deteriorated compared to the as received alloys and the alloy that was extruded at 350 °C. The formation of this layer decreased the corrosion via pitting attack as shown by the SEM image and also confirm the measured current vs. time behavior (Figure 7, curve 4), which recorded the lowest absolute values amongst all tested alloys. This indicates that the alloy that was extruded at 500 °C has the best performance against corrosion. The wt % for the elements detected on surface of the extruded alloy at 500 °C obtained by EDX spectrum, Figure 10, recorded the following; 62.73% Al, 29.54% O, 3.10% Si, 0.84% Fe, 0.31% Mg, 1.22% Na, and 2.26% Cl. The highest weight percentages were confirmed for Al and O, respectively and indicated that the main compound found on surface of the extruded alloy at 500 °C is an aluminum oxide. This oxide causes the protection of the surface of the surface of this alloy as aforementioned in CPP and EIS measurement sections. The presence of few pits on the surface of the alloy that was extruded at 500 °C compared to the number and width of pits found on the surfaces of the as received alloy (Figure 8) and the alloy that was extruded at 350 °C (Figure 9) proves the ability of the oxide film composed on the alloy extruded at 500 °C is more compact and protective than in its case for the as received alloy (Figure 8) and the alloy that was extruded at 350 °C (Figure 9).

4. Conclusions

A recycled AA6061 alloy device chip was extruded at 350, 425, and 500 °C. The influence of temperature on the corrosion of the extruded AA6061 chips was studied and compared to the corrosion of the as-received AA6061 alloy in 3.5% NaCl solutions. All CPP, EIS, and PCT measurements were consistent and in good agreement with each other revealing that the extrusion process greatly improves the corrosion resistance of AA6061 alloy and this effect gets enhanced with rising the extrusion temperature up to 500 °C. This is because raising the temperature increases the compactness of the protective layer of Al₂O₃ and thus increases the resistance to corrosion in the NaCl solution. The superior corrosion resilience of the recycled alloy that was extruded at 500 °C is associated to the effects of grain refinement, the existence of oxide contaminants, and the higher extrusion temperature. Prolonging the exposure time has also raised the resistance to corrosion, particularly the uniform corrosion type.

Author Contributions: Conceptualization, N.H.A. and E.-S.M.S.; methodology, E.-S.M.S. and A.T.A.; software, H.S.A.; validation, H.S.A., N.H.A. and E.-S.M.S.; formal analysis, E.-S.M.S., M.A.T. and N.H.A.; investigation, E.-S.M.S., H.F.A.; resources, N.H.A.; data curation, E.-S.M.S.; writing—original draft preparation, E.-S.M.S. and A.T.A.; writing—review and editing, N.H.A., E.-S.M.S. and H.F.A.; supervision, N.H.A. and E.-S.M.S. All authors have read and agreed to the published version of the manuscript.

Funding: The authors extend their appreciation to the Deanship of Scientific Research at King Saud University for funding this work through the research Project No NFG-15-03-08.

Conflicts of Interest: The authors declare no conflict of interest.

References

1. Badawy, W.A.; Al-Kharafi, F.M.; El-Azab, A.S. Electrochemical behaviour and corrosion inhibition of Al, Al-6061 and Al-Cu in neutral aqueous solutions. *Corros. Sci.* **1999**, *41*, 709–727. [[CrossRef](#)]
2. Szklarska-Smialowska, Z. Pitting corrosion of aluminum. *Corros. Sci.* **1999**, *41*, 1743–1767. [[CrossRef](#)]
3. Sherif, E.M.; Park, S.-M. Effects of 1,5-Naphthalenediol on Aluminum Corrosion as a Corrosion Inhibitor in 0.50 M NaCl. *J. Electrochem. Soc.* **2005**, *152*, B205. [[CrossRef](#)]
4. Foley, R.T.; Nguyen, T.H. Chemical nature of aluminum corrosion. *J. Electrochem. Soc.* **1982**, *129*, 464–467. [[CrossRef](#)]
5. Rangasamy Krishnan, V.P.; Subramanian, M. Electrodeposition of Ni-La₂O₃ composite on AA6061 alloy and its enhanced hardness, corrosion resistance and thermal stability. *Surf. Coat. Technol.* **2017**, *324*, 471–477. [[CrossRef](#)]
6. Shahidi, M.; Gholamhosseinzadeh, M.R. Electrochemical evaluation of AA6061 aluminum alloy corrosion in citric acid solution without and with chloride ions. *J. Electroanal. Chem.* **2015**, *757*, 8–17. [[CrossRef](#)]
7. Rosliza, R.; Wan Nik, W.B. Improvement of corrosion resistance of AA6061 alloy by tapioca starch in seawater. *Curr. Appl. Phys.* **2010**, *10*, 221–229. [[CrossRef](#)]
8. Zaid, B.; Saidi, D.; Benzaid, A.; Hadji, S. Effects of pH and chloride concentration on pitting corrosion of AA6061 aluminum alloy. *Corros. Sci.* **2008**, *50*, 1841–1847. [[CrossRef](#)]
9. Rosliza, R.; Senin, H.B.; Nik, W.B.W. Electrochemical properties and corrosion inhibition of AA6061 in tropical seawater. *Colloids Surf. A Physicochem. Eng. Asp.* **2008**, *312*, 185–189. [[CrossRef](#)]
10. Dadvand, N.; Caley, W.F.; Kipouros, G.J. Investigation of the corrosion behaviour of electroless nickel-phosphorus coatings on AA6061 in basic solutions. *Can. Metall. Q.* **2004**, *43*, 219–228. [[CrossRef](#)]
11. Haruna, T.; Kouno, T.; Fujimoto, S. Electrochemical conditions for environment-assisted cracking of 6061 Al alloy. *Corros. Sci.* **2005**, *47*, 2441–2449. [[CrossRef](#)]
12. Linardi, E.; Collet-Lacoste, J.; Lanzani, L. Characterization of AA6061 Alloy Oxides Obtained in High Purity Water and in Diluted NaCl Solution. *Procedia Mater. Sci.* **2015**, *8*, 56–64. [[CrossRef](#)]
13. Gronostajski, J.; Marciniak, H.; Matuszak, A. New methods of aluminium and aluminium-alloy chips recycling. *J. Mater. Proc. Technol.* **2000**, *106*, 34–39. [[CrossRef](#)]
14. Samuel, M. A new technique for recycling aluminium scrap. *J. Mater. Proc. Technol.* **2003**, *135*, 117–124. [[CrossRef](#)]
15. Ragab, A.E.; Taha, M.A.; Abbas, A.T.; Al Bahkali, E.A.; El-Danaf, E.A.; Aly, M.F. Effect of extrusion temperature on the surface roughness of solid state recycled aluminum alloy 6061 chips during turning operation. *Adv. Mech. Eng.* **2017**, *9*, 1687814017734152. [[CrossRef](#)]
16. Hunkeler, F.; Frankel, G.S.; Bohni, H. Technical Note: On the Mechanism of Localized Corrosion. *Corrosion* **1987**, *43*, 189–191. [[CrossRef](#)]
17. Mazhar, A.A.; Badawy, W.A.; Abou-Romia, M.M. Impedance studies of corrosion resistance of aluminium in chloride media. *Surf. Coat. Technol.* **1986**, *29*, 335–345. [[CrossRef](#)]
18. Wall, F.D.; Johnson, C.M.; Barbour, J.C.; Martinez, M.A. The Effects of Chloride Implantation on Pit Initiation in Aluminum. *J. Electrochem. Soc.* **2004**, *151*, B77. [[CrossRef](#)]
19. Sherif, E.M.; Park, S.-M. Effects of 1,4-naphthoquinone on aluminum corrosion in 0.50M sodium chloride solutions. *Electrochim. Acta* **2006**, *51*, 1313–1321. [[CrossRef](#)]
20. Sato, N. The stability of localized corrosion. *Corros. Sci.* **1995**, *37*, 1947–1967. [[CrossRef](#)]
21. Natishan, P.M.; O’Grady, W.E. Chloride Ion Interactions with Oxide-Covered Aluminum Leading to Pitting Corrosion: A Review. *J. Electrochem. Soc.* **2014**, *161*, C421–C432. [[CrossRef](#)]

22. Yağan, A.; Pekmez, N.Ö.; Yıldız, A. Corrosion inhibition by poly(N-ethylaniline) coatings of mild steel in aqueous acidic solutions. *Prog. Org. Coat.* **2006**, *57*, 314–318. [[CrossRef](#)]
23. Ramesh, C.S.; Keshavamurthy, R.; Naveen, G.J. Effect of extrusion ratio on wear behaviour of hot extruded Al6061–SiCp (Ni–P coated) composites. *Wear* **2011**, *271*, 1868–1877. [[CrossRef](#)]
24. Selmy, A.I.; El Aal, M.I.A.; El-Gohry, A.M.; Taha, M.A. Solid-State Recycling of Aluminum Alloy (AA-6061) Chips via Hot Extrusion Followed by Equal Channel Angular Pressing (ECAP). *Egypt. Int. J. Eng. Sci. Technol.* **2016**, *21*, 33–42.
25. Hu, M.; Ji, Z.; Chen, X.; Zhang, Z. Effect of chip size on mechanical property and microstructure of AZ91D magnesium alloy prepared by solid state recycling. *Mater. Charact.* **2008**, *59*, 385–389. [[CrossRef](#)]
26. Chino, Y.; Hoshika, T.; Mabuchi, M. Enhanced corrosion properties of pure Mg and AZ31Mg alloy recycled by solid-state process. *Mater. Sci. Eng. A* **2006**, *435–436*, 275–281. [[CrossRef](#)]
27. Chino, Y.; Hoshika, T.; Mabuchi, M. Mechanical and Corrosion Properties of AZ31 Magnesium Alloy Repeatedly Recycled by Hot Extrusion. *Mater. Trans.* **2006**, *47*, 1040–1046. [[CrossRef](#)]
28. Song, G.; StJohn, D. The effect of zirconium grain refinement on the corrosion behaviour of magnesium-rare earth alloy MEZ. *J. Light Met.* **2002**, *2*, 1–16. [[CrossRef](#)]
29. Gronostajski, J.Z.; Kaczmar, J.W.; Marciniak, H.; Matuszak, A. Direct recycling of aluminium chips into extruded products. *J. Mater. Process. Technol.* **1997**, *64*, 149–156. [[CrossRef](#)]
30. Sherif, E.-S.M. Effects of exposure time on the anodic dissolution of Monel-400 in aerated stagnant sodium chloride solutions. *J. Solid State Electrochem.* **2012**, *16*, 891–899. [[CrossRef](#)]
31. Ward, M.D. *Physical Electrochemistry*; Rubinstein, I., Ed.; Marcel Dekker: New York, NY, USA, 1995.
32. Khaled, K.F. Electrochemical investigation and modeling of corrosion inhibition of aluminum in molar nitric acid using some sulphur-containing amines. *Corros. Sci.* **2010**, *52*, 2905–2916. [[CrossRef](#)]
33. Mansfeld, F. Electrochemical impedance spectroscopy (EIS) as a new tool for investigating methods of corrosion protection. *Electrochim. Acta* **1990**, *35*, 1533–1544. [[CrossRef](#)]
34. Sherif, E.-S.M.; Potgieter, J.H.; Comins, J.D.; Cornish, L.; Olubambi, P.A.; Machio, C.N. Effects of minor additions of ruthenium on the passivation of duplex stainless-steel corrosion in concentrated hydrochloric acid solutions. *J. Appl. Electrochem.* **2009**, *39*, 1385–1392. [[CrossRef](#)]
35. AlHazaa, A.N.; Sherif, E.S.M.; Abdo, H.S. Galvanic corrosion in 3.5 wt. % NaCl solutions of magnesium alloy AZ31 coupled with Ni after different bonding periods of time. *Int. J. Electrochem. Sci.* **2015**, *10*, 5420–5433.
36. Sherif, E.-S.M.; Erasmus, R.M.; Comins, J.D. In situ Raman spectroscopy and electrochemical techniques for studying corrosion and corrosion inhibition of iron in sodium chloride solutions. *Electrochim. Acta* **2010**, *55*, 3657–3663. [[CrossRef](#)]

